A New Method to Detect the High Impedance Dipole Modes of TESLA Cavities

Stéphane Fartoukh
DAPNIA/SEA,
CEA/Saclay F-91191 Gif sur Yvette Cedex, France

June 2, 1998

Abstract

In the aim of detecting or classifying the resonant and trapped dipole modes of TESLA cavities and in order to measure their quality factors, two different beam experiments have been already proposed [1, 2]. Presently, the latter cannot be carried out since both require a beam the characteristics of which are the ones of the future TTF injector, Injector II (8 nC bunches, repetition frequency of 1 MHz). The aim of this paper is then to introduce the idea of a new beam experiment consisting in modulating the bunch charge at a certain frequency Ω, feasible with the present TTF injector (bunch repetition frequency of 216 MHz with an average beam current of about 10 mA) and permitting to produce, with an equivalent sensitivity, the same measurements as the ones previously mentioned.

1 Introduction and Recalls

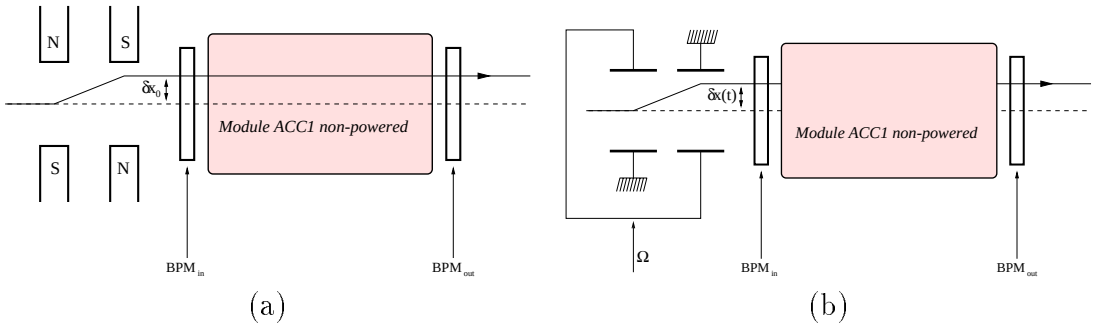

Figure 1: (a): Experiment I; (b): Experiment II

We begin here the discussion by a brief recall concerning the two beam experiments currently proposed for the measurement of the long-range dipole wakefields generated in the TESLA cavities. We invite the reader to consult Ref. [3] for a more detailed introduction and insist on the fact that, for evident reasons reported hereafter, these two experiments are not in any case feasible with the present TTF injector, Injector I.
The first experiment (Experiment I, A. Mosnier [1]) consists in injecting the beam 10 mm off-axis into the first non-powered 8-cavity module and monitoring the bunch position at its exit (see Fig. 1(a)). Let us now assume that the eigenfrequency $\omega_{\alpha,i}$ associated to the dipole mode α of the i^{th} cavity verifies the resonance condition,

$$\omega_{\alpha,i} = n\,\omega_b\,(1 \pm 1/2Q_{\alpha,i})\ , \tag{1}$$

where n is any integer and where ω_b and $Q_{\alpha,i}$ represents the bunch repetition frequency and the quality factor of the considered mode respectively; in this case, it can be shown that the transverse beam displacement is amplified at the BPM location by an amount which is proportional to the initial train offset δx_0, the average current I_b divided by the injection energy E_0 and the shunt impedance $R_{\alpha,i}$ of the selected mode (in the following expression, the short-range wakefield contribution is omitted):

$$\delta x_{\text{BPM}} - \delta x_0 = \mathbf{Cst_1}\ \times\ \delta x_0\,\frac{I_b}{E_0}\,R_{\alpha,i}\ . \tag{2}$$

In order to reproduce experimentally the resonance condition 1, the geometry of one or several cavities has to be modified during the experiment which is made possible by the fact that they are not powered; it is then sufficient to actuate the tuning system of the selected cavities, and in a relatively short range since the bunch repetition frequency will be equal to 1 MHz with Injector II: with the beam delivered by the present TTF injector for which $\omega_b = 216$ MHz, the frequency ranges which have to be explored becomes to wide, which made this experiment un-feasible. Finally, concerning the Injector II beam, note

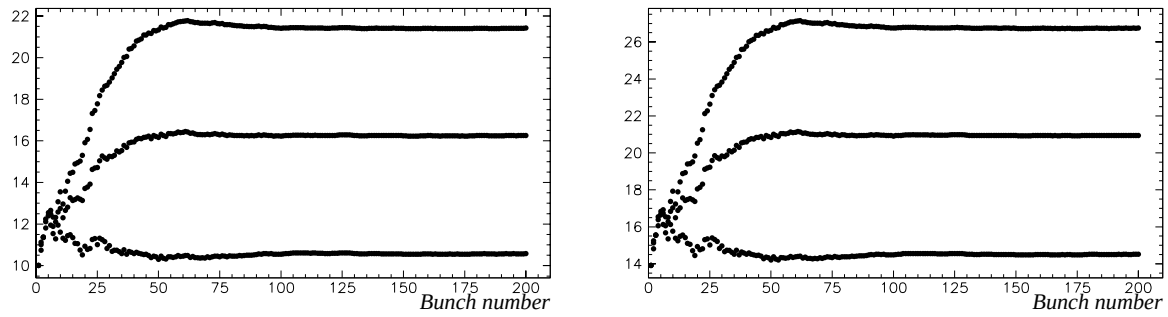

(a) (b)

Figure 2: Experiment I. Bunch position [mm] at the exit of module ACC1 without (a) and with (b) single-bunch beam breakup. 0, 1 or 2 cavities tuned to the TM110_5 mode ($(R/Q) \times Q = 10^{10}\,\Omega/\mathrm{m}^2$, $\omega \sim 1875$ MHz); 8 nC bunch charge, injection energy of 20 MeV, bunch train injected 10 mm off-axis, cavities un-powered.

that the short and long-range dipole wakefield effects are of the same order of magnitude and become then coupled (contributions of 4, 4.7, 5.3 mm for the short-range wakefields against 0.5, 6.3, 11.5 mm for the long-range ones when zero, one or two cavities are tuned to the TM110_5 mode respectively, compare Fig. 2(a) and 2(b)), which could deteriorate the measurement quality. With Injector I, this difficulty disappears, since the bunch charge is divided by a factor 216.

In the second experiment (Experiment II, V. Balakin [2]), the method proposed consists in modulating with time the initial transverse coordinates of bunches at the frequency Ω. By operating with a pair of rf deflectors (see Fig. 1(b)), the bunch number n goes into the first cryomodule with the following initial conditions:

$$\delta x_{n,0} = \delta x_0 \, \sin(n\,\Omega\,T_b + \phi) \quad \text{and} \quad \delta x'_{n,0} = 0 \tag{3}$$

where $T_b \stackrel{\text{def}}{=} 2\pi/\omega_b$ and $0 \leq \Omega < \omega_b/2$ (first half-Brillouin zone). As previously, it is better that the cavities are not powered in order to maximize the signal amplitude obtained at the output BPM location, but it is not a absolute necessity. Under these conditions, it can be shown [3] that the transverse displacement of bunch number n is given by the following expression at the output BPM location:

$$\delta x_{n,\mathrm{BPM}} - \delta x_{n,0} = \delta x_0 \left(\mathbf{A}_+(\Omega) \, \sin(n\,\Omega\,T_b + \phi) - \mathbf{A}_-(\Omega) \, \cos(n\,\Omega\,T_b + \phi) \right) . \tag{4}$$

Now, given a dipole mode of frequency $\omega_{\alpha,i}$, if the modulation frequency Ω verifies the condition,

$$\omega_{\alpha,i} \pm \Omega_{res} = n\,\omega_b \ , \ n \text{ integer} \ , \tag{5}$$

then the in-phase component $\mathbf{A}_+(\Omega)$ is quasi-vanishing while the component in quadrature $\mathbf{A}_-(\Omega)$ exhibits a resonance the magnitude of which is proportional, as previously, to the

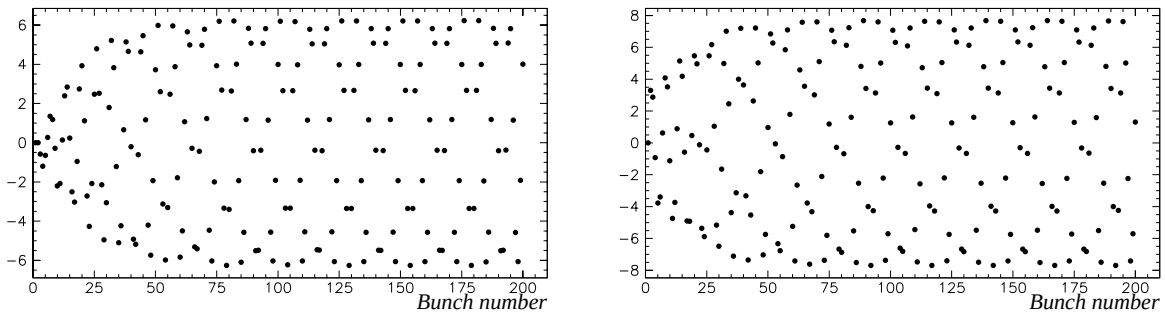

(a) (b)

Figure 3: Experiment II. Relative bunch displacement [μm] (i.e. difference between the output signal and the input one) at the exit of module ACC1 without (a) and with (b) single-bunch beam breakup effect. The modulation frequency Ω is tuned to the resonance condition of the TM110_5 mode of the first cavity; 8 nC bunch charge, injection energy of 20 MeV, $\delta x_0 = 10\mu$m, cavities un-powered.

initial amplitude modulation δx_0, the average current I_b divided by the injection energy E_0 and the shunt impedance $R_{\alpha,i}$ of the selected mode:

$$\mathbf{A}_+ (\Omega_{res}) \approx 0 \quad \text{and} \quad \mathbf{A}_- (\Omega_{res}) = \mathbf{Cst_2} \times \delta x_0 \frac{I_b}{E_0} R_{\alpha,i} \tag{6}$$

with $\mathbf{Cst_2} = \mathbf{Cst_1}$ (see Eq. 2). From this point of view, Experiments I and II have rigorously the same sensitivity. In fact, the rf deflectors represented on Fig. 1(b) can only achieve a modulation amplitude of 10 μm [4] so that the expected resonance magnitudes will be divided by a factor 1000 in comparison with Experiment I (see Fig. 3, now the scale is in microns).
However that may be, by assuming the output BPM to possess an good enough resolution and by using robust signal analysis methods (in order to extract from the output signal the short-range wakefield contribution as well as the noise coming from the bunch to bunch jitter), one can theoretically scan all the frequencies of the most dangerous dipole modes (i.e the ones of highest impedances) by varying the modulation frequency Ω between 0 and $\omega_b/2$, i.e. between 0 and 0.5 MHz considering the Injector II beam parameters. Now, if the same experiment had to be carried out with the Injector I beam, the variation range of Ω should be 0-108 MHz, which would require to use enormous deflecting rf cavities, certainly too costly.

Before closing this section, it is also important to insist on the following fact. In the relevant variation range of Ω (0-0.5 MHz), about a hundred of resonances are expected at the output BPM location corresponding to the highest impedance dipole modes of the eight cavities of the first cryomodule. These resonances having widths of a few tens of kHz (associated to the band widths $\omega_{\alpha,i}/Q_{\alpha,i}$ of the modes considered), the measurement interpretation could then become extremely tricky due to numerous overlappings of the peaks observed. In order to illustrate this situation, the functions $\mathbf{A}_+(\Omega)$ and $\mathbf{A}_-(\Omega)$ have

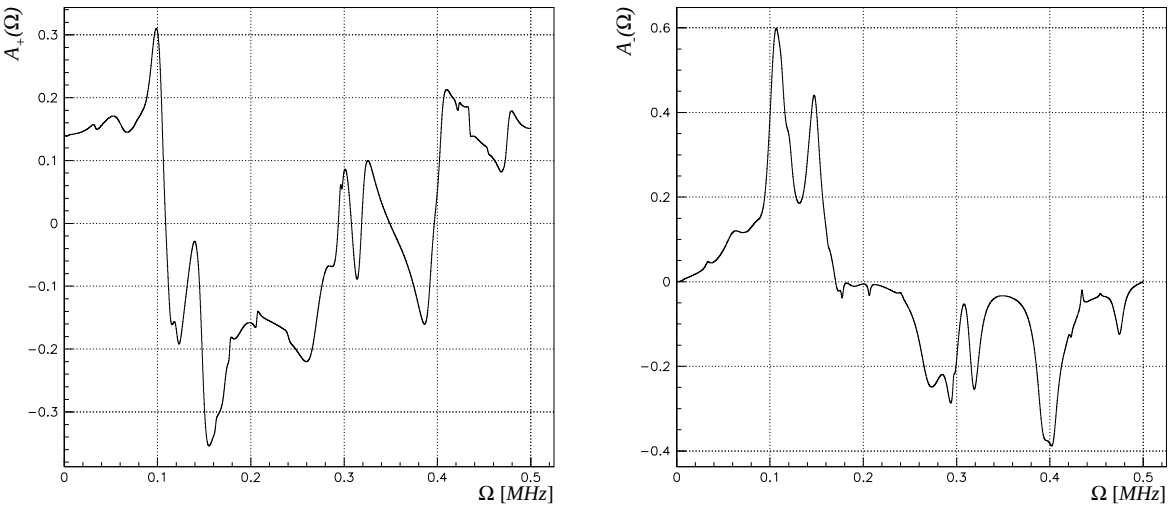

Figure 4: Experiment II. Response functions $\mathbf{A}_+(\Omega)$ and $\mathbf{A}_-(\Omega)$ versus Ω [MHz]; 8 nC bunch charge, injection energy of 20 MeV, bunch repetition frequency of 1 MHz (Injector II), cavities un-powered.

been plotted in Fig. 4. These simulations have been made considering the ten highest impedance dipole modes of TESLA cavities (see Ref. [5, Tab. 4.6]). For each of them, the quantities $(R/Q)_{\alpha,i}$ and $Q_{\alpha,i}$ have been taken independent of the number i of the cavity considered whereas a spread of 1 MHz (from cavity to cavity) in the frequencies $\omega_{\alpha,i}$ has been taken into account. The response function $\mathbf{A}_-(\Omega)$ should then exhibit about 80 peaks in the range 0-0.5 MHz which are far from being readable on Fig. 4. Incidentally, note that the response function $\mathbf{A}_-$ reaches its maximum value for $\Omega \approx 0.1$ MHz, $\mathbf{A}_-^{peak} = 0.6$. This number corresponds to the mode TM110_5 of the first ACC1 cavity as shown previously in Fig. 3(a).

2 Experiment III: scanning of dipole modes by modulating the bunch charge

Although Experiment II presents the main three drawbacks previously mentioned (initial modulation amplitude of only 10 μm, strong contribution of the short-range wakefields, resonance overlapping due to the relatively small bunch repetition frequency of Injector II), it remains nevertheless quite interesting, especially if it was possible to realize it with the presently installed TTF injector, Injector I (which is not the case as explained before). The idea is then, not to study the feasibility of this kind of experiment with the Injector I beam, but rather to conceive an experimental situation which would be able to reproduce artificially the multi-bunch effects generated in Experiment II (with the possibility to have a variation range of Ω between 0 and 108 MHz).

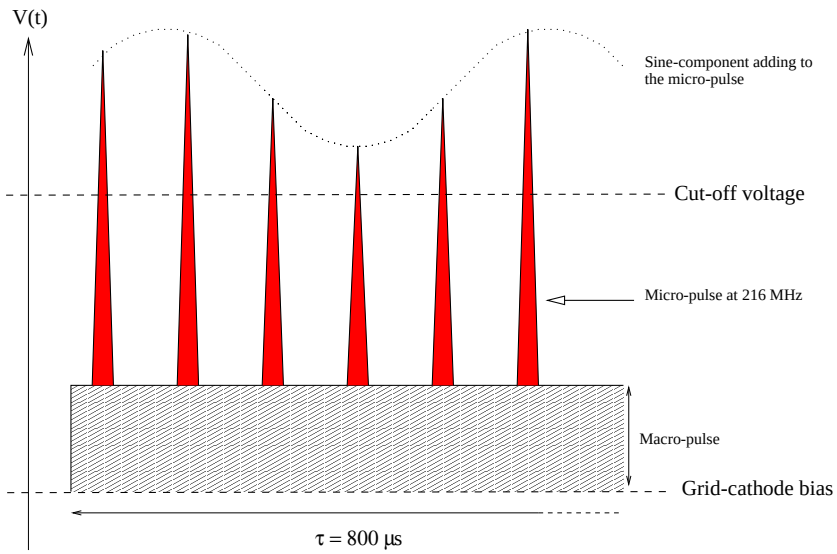

Figure 5: Modulation with time of the micro-pulse voltage

2.1 Description

The principle is the following:

- inject the bunch train 10 mm off-axis using the dog-leg planned for Experiment I (see Fig. 1(a)).
- modulate with time the bunch charge at a frequency Ω between 0 and 108 MHz, by adding a sine-component to the micro-pulse voltage (see Fig. 5).

It is then necessary to know the variation of the bunch charge as a function of the voltage exceeding the one of the grid-cathode cut-off tension. A first preliminary experiment recently done on TTF has shown that this dependence is quasi-linear in the range of current 2-10 mA [6] (see Fig. 6). Moreover, it has been also verified that the modulation with time of the micro-pulse amplitude was quite feasible [7].
Under these conditions, it seems then reasonable to think that Injector I should be able to generate bunch trains having the following characteristics at the first module entrance:

$$\begin{cases} \delta x_{0,n} = \delta x_0 = 10\,\mathrm{mm} & \\ \delta x'_{0,n} = 0 & 1 \leq n \leq 800 \times 216 \\ Q_{b_n} = Q_{b_0}\Big(1 + \lambda \sin(n\Omega T_b + \phi)\Big) & 1 \leq n \leq 800 \times 216 \end{cases} \tag{7}$$

where Ω between 0 and 108 MHz, $Q_{b_0} = 8/216$ nC and $T_b = 1/216\,\mu$s, giving an average beam current of 8 mA as for Injector II, and where the amplitude λ has to be defined carefully because, as we will see, it is one of the main parameters which acts upon the measurement sensitivity. A possible choice for λ is 0.5 giving a modulation of the local current between 4 and 12 mA (range in which the bunch charge is effectively linear with

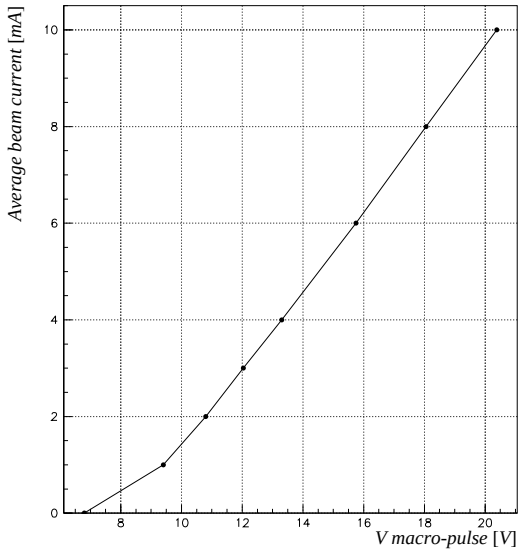

Average beam current [mA]	V macropulse [V]
10	20.38
8	18.05
6	15.75
4	13.3
3	12.03
2	10.8
1	9.4
0	6.8

Figure 6: Beam current variation as a function of the macro-pulse voltage [6]

respect to the micro-pulse voltage as shown by the probable extrapolation of Fig. 6 up to 12 mA).
In the next paragraph, we will then show that this situation simulates completely an experiment of type II carried out with the present TTF injector and for which the equivalent modulation amplitude of the transverse bunch position is equal to $\lambda \cdot \delta x_0$ (i.e 5 mm to be compared with the 10 μm previously proposed). Moreover, since, in the present case, the bunch charge is divided by more than two orders of magnitude and since the relevant variation range of Ω goes from 0-0.5 MHz to 0-108 MHz, the short-range wakefield effects disappear quite simply as well as the problems of resonance overlapping.

2.2 Resonance conditions and amplification coefficients

We begin the discussion by considering a bunch train of energy E_0, presenting the characteristics described by Eq. 7 and going through the non-powered TTF cavity number i. We note W_{T_i} [V/C/m/structure] the long-range dipole wakefield per structure and unit charge generated in the cavity considered:

$$W_{T_i}(z) = 2\sum_{\alpha} \frac{k_{\alpha,i}\, c}{\omega_{\alpha,i}\, a^2} \sin(\omega_{\alpha,i}\, z/c)\ \exp(-z/z_{\alpha,i})\ , z > 0$$

$$\text{with} \begin{cases} k_{\alpha,i} \stackrel{\text{def}}{=} \dfrac{\omega_{\alpha,i}}{4} \left(\dfrac{R}{Q}\right)_{\alpha,i} & \text{(loss factor per structure [V/C/structure])} \\ z_{\alpha,i} \stackrel{\text{def}}{=} c\ \dfrac{2Q_{\alpha,i}}{\omega_{\alpha,i}} & \text{(damping length [m] of mode } \alpha) \end{cases} \quad (8)$$

where a is the iris aperture radius. At the exit of this cavity, the bunch number n is then subjected to a kick noted $\delta x'_{n,i}$ and given by the expression,

$$\delta x'_{n,i} = \delta x_0 \frac{e}{E_0} \sum_{k=0}^{n-1} Q_{b_k} W_{T_i}\Big((n-k)\lambda_b\Big) \ , \tag{9}$$

where $\lambda_b = cT_b = 2\pi c/\omega_b$ represents the distance between two consecutive bunches. Finally, by using the expressions of Q_{b_k} and W_{T_i} and after some algebra, we can show that after a transient regime (associated to the maximum damping length $z_{\alpha,i}$, that is about 150×216 bunches for Injector I) the quantity $\delta x'_{n,i}$ takes the following form:

$$\begin{aligned}\delta x'_{n,i} \overset{n\to\infty}{\approx} \delta x_0 \frac{eQ_{b_0}}{E_0}\frac{c}{2a^2}\Bigg\{ &\left[\sum_\alpha \left(\frac{R}{Q}\right)_{\alpha,i} p_r(\omega_{\alpha,i}, Q_{\alpha,i}, T_b)\right] + \\ &\lambda\Bigg(\left[\sum_\alpha \left(\frac{R}{Q}\right)_{\alpha,i} \mathcal{A}_+(\omega_{\alpha,i}, Q_{\alpha,i}, T_b, \Omega)\right]\sin(n\Omega T_b + \phi) - \\ &\left[\sum_\alpha \left(\frac{R}{Q}\right)_{\alpha,i} \mathcal{A}_-(\omega_{\alpha,i}, Q_{\alpha,i}, T_b, \Omega)\right]\cos(n\Omega T_b + \phi)\Bigg)\Bigg\}\end{aligned} \tag{10}$$

where the analytical expressions of the amplitudes p_r and $\mathcal{A}_\pm$ are given hereafter:

$$\begin{aligned} p_r(\omega, Q, T_b) &\overset{\text{def}}{=} \frac{1}{2}\frac{\sin(\omega T_b)}{\cosh\left(\frac{\omega T_b}{2Q}\right) - \cos(\omega T_b)} \\ \mathcal{A}_+(\omega, Q, T_b, \Omega) &\overset{\text{def}}{=} \frac{1}{2}\frac{\sin(\omega T_b)\left(\cosh\left(\frac{\omega T_b}{2Q}\right)\cos(\Omega T_b) - \cos(\omega T_b)\right)}{\left(\cosh\left(\frac{\omega T_b}{2Q}\right) - \cos(\omega T_b - \Omega T_b)\right)\left(\cosh\left(\frac{\omega T_b}{2Q}\right) - \cos(\omega T_b + \Omega T_b)\right)} \\ \mathcal{A}_-(\omega, Q, T_b, \Omega) &\overset{\text{def}}{=} \frac{1}{2}\frac{\sin(\omega T_b)\sinh\left(\frac{\omega T_b}{2Q}\right)\sin(\Omega T_b)}{\left(\cosh\left(\frac{\omega T_b}{2Q}\right) - \cos(\omega T_b - \Omega T_b)\right)\left(\cosh\left(\frac{\omega T_b}{2Q}\right) - \cos(\omega T_b + \Omega T_b)\right)} \ . \end{aligned} \tag{11}$$

The study of these three functions has already been done in Ref. [3] (for the beam parameters of injector II, i.e $\omega_b = 1$ MHz) and is reported hereafter including the case where $\omega_b = 216$ MHz (Injector I)

- The response function p_r (independent of the modulation frequency Ω) is of course rigorously the same as the one occurring in Experiment I (making $\lambda = 0$ in Eq. 7, we retrieve exactly the same initial conditions as the ones of Experiment I). For a given dipole mode ω, the latter is quasi-null except if the mode considered verifies the resonance condition 1 (i.e ω closed to an integer multiple of the bunch repetition frequency). In this case, the function $p_r(\omega)$ reaches its peak value (see Fig. 7):

$$p_r^{peak} = \pm\frac{\omega_b}{\omega}\frac{Q}{2\pi} \ \text{ if } \ \omega = n\omega_b\left(1 \pm \frac{1}{2Q}\right) \tag{12}$$

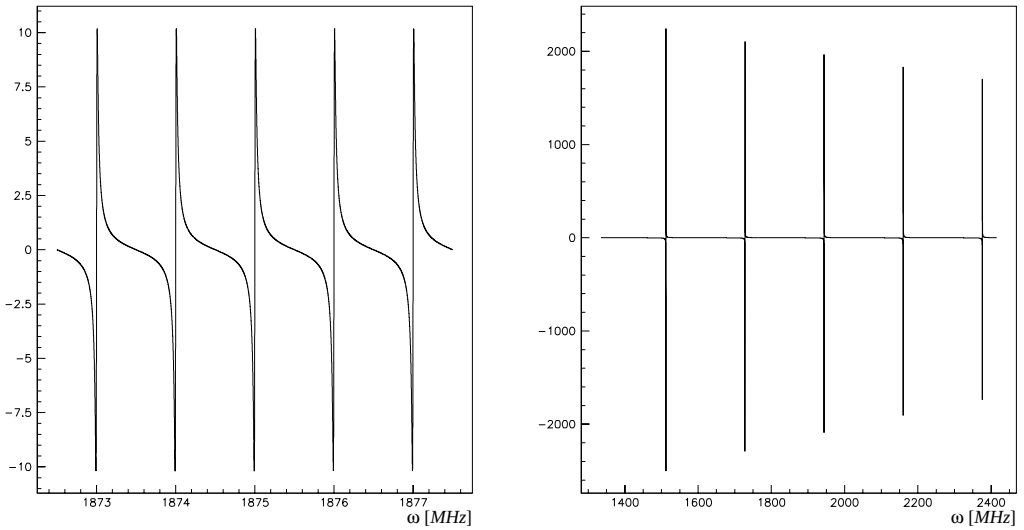

(a) (b)

Figure 7: Function p_r versus ω [MHz] for $\omega_b = 1$ MHz (a) and $\omega_b = 216$ MHz (b), $Q = 1.2\,10^5$

where n is any integer and where Q is the quality factor of the mode considered.

- The response functions $\mathcal{A}_\pm$ are exactly the same than the ones occurring in Experiment II. Indeed, from a mathematical point of view, the long-range wakefields generated by bunches injected with the same offset but the charge of which is modulated with time are rigorously the same as the ones produced by bunches of constant charge but the initial transverse positions of which are oscillating at the frequency Ω considered.

This being said, for a given dipole mode (ω and Q fixed), we can easily check that these functions are of period ω_b with the modulation frequency Ω; $\mathcal{A}_+$ and $\mathcal{A}_-$ are symmetrical and anti-symmetrical respectively with respect to $\omega_b/2$, so that the relevant variation range of Ω is 0-$\omega_b/2$, i.e. 0-108 MHz for Injector I. The function $\mathcal{A}_-$ reaches its peak value when $\omega \mp \Omega_{res}$ is an integer multiple of the bunch repetition frequency (Ω_{res} being chosen in the range 0-$\omega_b/2$), in which case $\mathcal{A}_+$ is vanishing:

$$\mathcal{A}_-\Big(\Omega_{res}\Big) = \mathcal{A}_-^{peak} \equiv p_r^{peak} = \pm\,\frac{\omega_b}{\omega}\,\frac{Q}{2\pi} \quad \text{and} \quad \mathcal{A}_+\Big(\Omega_{res}\Big) = 0 \quad \text{where} \quad \omega \mp \Omega_{res} = n\omega_b \ . \tag{13}$$

Inversely, the amplification $\mathcal{A}_+$ possesses two opposite extrema on either side of Ω_{res}, for $\Omega = \Omega_{res} \mp \omega/(2Q)$; on these points the functions $\mathcal{A}_+$ and $\mathcal{A}_-$ are identical and equal (in absolute value) to $\mathcal{A}_-^{peak}/2$:

$$\mathcal{A}_+\Big(\Omega_{res} \mp \omega/(2Q)\Big) = \pm\,\frac{\mathcal{A}_-^{peak}}{2} \quad \text{and} \quad \mathcal{A}_-\Big(\Omega_{res} \mp \omega/(2Q)\Big) = \frac{\mathcal{A}_-^{peak}}{2} \ . \tag{14}$$

These functions are plotted in Fig. 8 for $\omega_b = 1$ MHz and $\omega_b = 216$ MHz, considering the most dangerous dipole mode of TESLA cavities, the mode TM110_5 of frequency $\omega = 1874.8 \sim (9\times216 - 69)$ MHz (giving $\Omega_{res} \sim 69$ MHz for $\omega_b = 216$ MHz and $\Omega_{res} = 0.2$ MHz for $\omega_b = 1$ MHz) and of quality factor $Q = 1.2\,10^5$ (BBU limit).

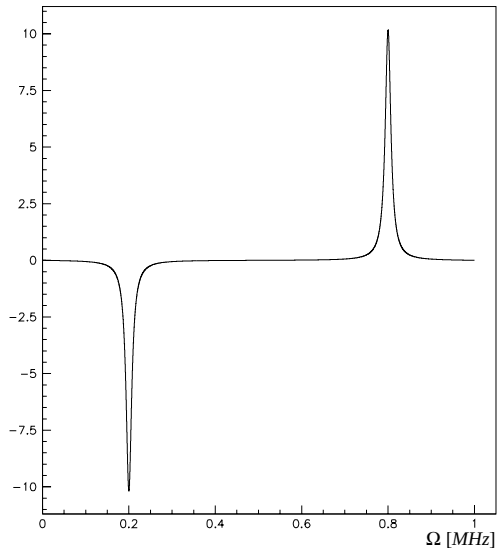

(a): $\mathcal{A}_-$ vs Ω for $\omega_b = 1$ MHz

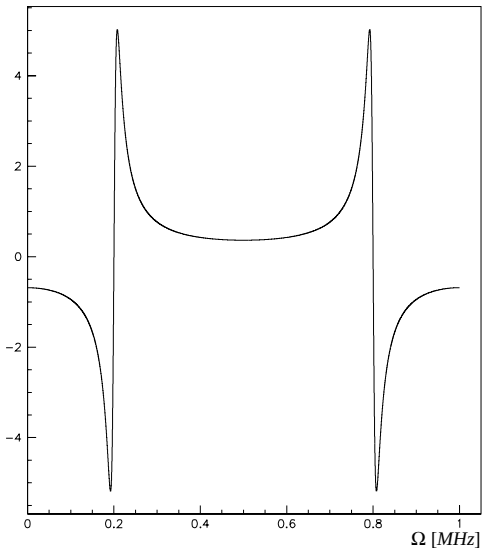

(b): $\mathcal{A}_+$ vs Ω for $\omega_b = 1$ MHz

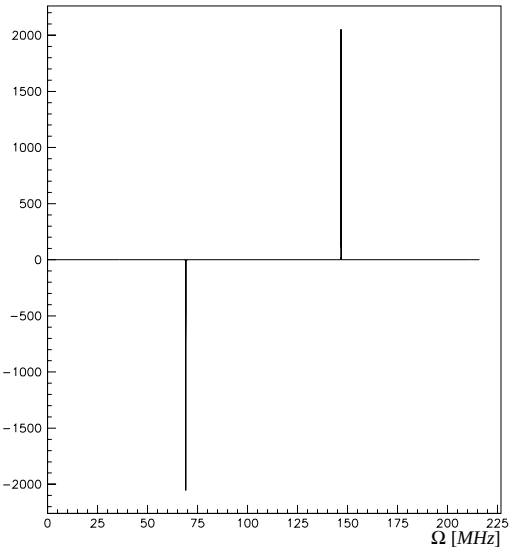

(c): $\mathcal{A}_-$ vs Ω for $\omega_b = 216$ MHz

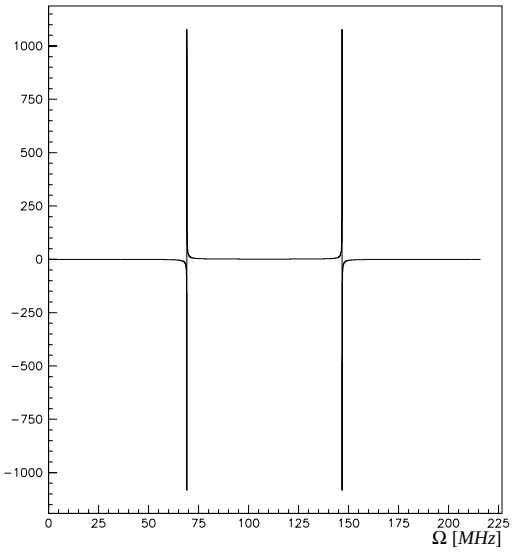

(d): $\mathcal{A}_+$ vs Ω for $\omega_b = 216$ MHz

Figure 8: Response functions $\mathcal{A}_\pm$ versus Ω [MHz] for $\omega_b = 1$ MHz (a)-(b) and $\omega_b = 216$ MHz (c)-(d), $Q = 1.2\,10^5$, $\omega = 1874.8$ MHz

Let us continue the discussion by computing the transverse position of bunch n at the output BPM location. By noting L_i the distance from the exit of cavity number i to the output BPM and using Eq. 10, this displacement is given by

$$\begin{aligned} \delta x_{n,\mathrm{BPM}} &= \delta x_0 + \sum_{i=1}^{8} \delta x'_{n,i}\, L_i \\ &\overset{n\to\infty}{\sim} \delta x_0 \Big(1 + \mathbf{P_r} + \lambda\big[\mathbf{A}_+(\Omega)\,\sin(n\Omega T_b + \phi) - \mathbf{A}_-(\Omega)\,\cos(n\Omega T_b + \phi)\big]\Big) \end{aligned} \tag{15}$$

$$\text{where} \quad \begin{cases} \mathbf{P_r} \\ \mathbf{A}_\pm(\Omega) \end{cases} \overset{\text{def}}{=} \frac{eQ_{b_0}}{E_0}\,\frac{c}{2a^2} \sum_{\alpha,i} \left[L_i \left(\frac{R}{Q}\right)_{\alpha,i} \times \begin{cases} p_r(\omega_{\alpha,i}, Q_{\alpha,i}, T_b) \\ \mathcal{A}_\pm(\omega_{\alpha,i}, Q_{\alpha,i}, T_b, \Omega) \end{cases} \right] . \tag{16}$$

As announced before, it is clear that the functions $\mathbf{A}_\pm(\Omega)$ occurring in the preceding equation are also the ones of Eq. 4. Moreover, by assuming the frequencies $\omega_{\alpha,i}$ not to be closed to an integer multiple of the bunch repetition frequency (in a range of a few tens of kHz), which is quite unlikely for $\omega_b = 216$ MHz, the quantity $\mathbf{P_r}$ is expected to be very small. Therefore, the absolute amplification of the signal read at BPM is theoretically identical to the one which would be obtained by an experiment of type II carried out with the Injector I beam and for which the initial modulation amplitude of the transverse bunch position would be equal to $\lambda \cdot \delta x_0 = 5$ mm. Thus, since the beam energy at the exit of the capture cavity is two times smaller with Injector I than it is with injector II, the sensitivities of Experiments I and III are rigorously the same, 1000 times higher than the one of Experiment II (carried out with the beam of Injector II)!

2.3 Simulations

Injection energy	$E_0 = 10\,\mathrm{MeV}$
Bunch repetition frequency	$\omega_b = 216\,\mathrm{MHz}$
Average beam current	$I_b = 8\,\mathrm{mA}$
Injection offset	$\delta x_0 = 10\,\mathrm{mm}$
Relative amplitude of the charge modulation	$\lambda = 0.5$
Variation range of the modulation frequency	$0 - 108\,\mathrm{MHz}$
Bunch charge	$4/216 - 12/216\,\mathrm{nC}$

Table 1: Beam parameters for Experiment III

The response functions $\mathbf{A}_\pm$ defined by Eq. 16 are plotted in Fig. 9 for the beam parameters of Injector I and a transverse displacement of the train of 10 mm at the dog-leg exit (see Tab. 1). The ten transverse modes of highest impedances used for this computation are taken from Ref. [5, Tab. 4.6]. They are reported in Tab. 2, classified in decreasing order of impedance; the frequencies Ω_{res} corresponding to the resonance conditions 5 are also

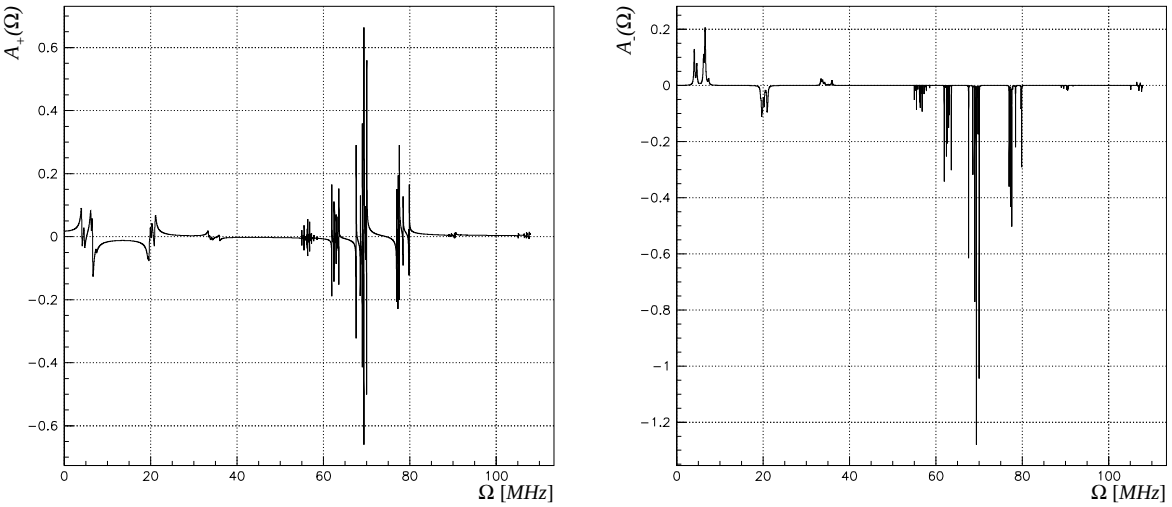

Figure 9: Experiment III. Response functions $\mathbf{A}_+(\Omega)$ and $\mathbf{A}_-(\Omega)$ versus Ω [MHz]; 8/216 nC average bunch charge, injection energy of 10 MeV, bunch repetition frequency of 216 MHz (Injector I), cavities un-powered.

Mode	Freq. [MHz]	$\frac{1}{a^2}\left(\frac{R}{Q}\right)$ [Ω/cm^2]	Q (BBU limit)	Impedance [Ω/cm^2]	Ω_{res} [MHz]
TM110_5	1874.8	8.75	$1.20\,10^5$	$1.05\,10^6$	69.2
TM110_4	1865.5	6.47	$7.60\,10^4$	$4.92\,10^5$	78.5
TM110_6	1881.2	1.83	$1.94\,10^5$	$3.56\,10^5$	62.8
TM110_8	1887.8	0.18	$6.70\,10^5$	$1.21\,10^5$	56.2
TE111_7	1734.3	15.4	$7.50\,10^3$	$1.16\,10^5$	6.30
TE111_6	1707.8	10.0	$8.10\,10^3$	$8.10\,10^4$	20.2
TM110_7	1885.4	0.10	$3.30\,10^5$	$3.30\,10^4$	58.6
TM110_2	1837.0	0.45	$4.70\,10^4$	$2.12\,10^4$	107.
TM110_3	1853.2	0.33	$5.20\,10^4$	$1.72\,10^4$	90.8
TE111_8	1762.2	2.23	$7.40\,10^3$	$1.66\,10^4$	34.2

Table 2: Highest impedance dipole modes of TESLA cavities

specified (for $\omega_b = 216$ MHz). Finally, for a given transverse mode ω, a frequency spread of 1 MHz (from cavity to cavity) had be included in these simulations. The expected resonances are then completely readable on Fig. 9 (compare with Fig. 4) with perhaps a slight overlapping of modes TM110_7 and TM110_8 for which $\Omega_{res} = 58.6$ and 56.2 MHz respectively (cf. Tab. 2). As expected, the response function $\mathbf{A}_-$ reaches its peak value for $\Omega \sim 70$ MHz; this resonance corresponds to the highest impedance transverse mode TM110_5 and is about two times higher than the one occurring in Fig. 4 since the beam injection energy has been divided by a factor of two.

2.4 Monitoring

To summarize, the signal obtained at the output BPM location possesses the following form:

$$\left\{ \begin{array}{rcl} Q_b(t) & = & \Theta(t)\, Q_{b_0} \Big(1 + \lambda\, \sin(\Omega t + \phi)\Big) \\ \delta x(t) & = & \Theta(t)\, \delta x_0 \left(1 + \mathbf{P_r} + \lambda \Big[\mathbf{A}_+(\Omega)\, \sin(\Omega t + \phi) - \mathbf{A}_-(\Omega)\, \cos(\Omega t + \phi)\Big]\right) \end{array} \right. \tag{17}$$

where $\Theta(t) \stackrel{\text{def}}{=} \sum_n \delta(t - nT_b)$ and where $\mathbf{P_r} \approx 0$ ($\mathbf{P_r} = 0.014$ in the simulations done in the previous paragraph) is independent of the modulation frequency Ω. Now, we have to envisage the two following situations:

- the BPM used for this experiment possesses a large pass-band ($\gtrsim \omega_b \sim 200\,$MHz), in which case the complete reconstruction of the signal is feasible.
- the BPM pass-band is only of a few MHz (presently 2 MHz for the BPM of type resonating cavity located at the exit of module ACC1), in which case the latter is only sensitive to the average value of $Q_b\, \delta x$, and then only to the response function $\mathbf{A}_+$:

$$\frac{\langle Q_b \delta x \rangle}{Q_{b_0}} \approx \delta x_0 \left(1 + \mathbf{P_r} + \frac{\lambda}{2}\, \mathbf{A}_+(\Omega)\right) \ . \tag{18}$$

  Since the peak values of $\mathbf{A}_+$ are two times smaller than the ones of the response function $\mathbf{A}_-$, a factor of $4/\lambda = 8$ is lost in the measurement sensitivity.

As said here above, the BPM susceptible to be used for this experiment possesses a pass-band of 1-2 MHz. The possibility to replace it is presently under investigation.

3 Conclusions

To conclude, I hope to have convinced my colleagues of the feasibility and the advantages of this beam experiment by comparison with the ones already proposed. The three main issues to be solved are the following:

- 1. implement the electronics required for the modulation of the micro-pulse voltage.
- 2. install the dog-leg (which is already constructed).
- 3. discuss the type of BPM to be used for this experiment (small or large pass-band).

Acknowledgments

Thanks to M. Jablonka and J.M. Joly for useful discussions concerning the feasibility study of this experiment, to B. Aune, A. Mosnier and O. Napoly for pertinent comments.

References

[1] A. Mosnier. *Instabilities in Linacs.* CERN 95-06, Rhodes, Greece, Sep. 1995, p. 459.

[2] V. Balakin. *Proposal for an Experiment at Tesla Test Facility.* Communication, March 1996, Protvino.

[3] S. Fartoukh. Multi-bunch experiment on TTF. DAPNIA/SEA-98-04 and TESLA-Note 98-07, Feb. 1998.

[4] V. Balakin. *Private communication.* TTF meeting at DESY, March 9-11, 1998.

[5] TESLA collaboration. *TESLA test facility linac - Design Report.* Version 1.0, March 1995, TESLA Report 95-01.

[6] J.M. Joly. Private communication, Desy, Ap. 1998.

[7] J.M. Joly, M. Bernard. Private communication, Orsay, Ap. 1998.